

The airplane crash at the “Pirelli” tall building

A. Franchi, A. Migliacci, M. Acito & P. Crespi

Politecnico di Milano, Milan, Italy

ABSTRACT: This paper is meant to deliver an overview on the damages and the following repairs of the structures of the 26th and 27th floor due to the airplane accident occurred on April, the 18th 2002. An aircraft 112 TC Commander impacted the facade of the Pirelli skyscraper getting into the building, where its gasoline tanks exploded. The first part of the paper focuses on a simplified analysis with the aims of evaluating the blast impulse and the peak pressure caused by the explosion on the floors structures. Then, a description of the realignment of the deck and the repairing operations are briefly summarized.

1 PREMISES

On 18 April 2002, at 17.47 hours, a 112 TC Commander single-engine plane struck the facade of the Pirelli skyscraper overlooking Piazza Duca d’Aosta (Fig. 1) between the deck beams of the 26th floor and those of the 27th floor, near the central cross-section, penetrating inside the building (Figs 2-4).

As the result of the collision and the explosion of the two fuel-tanks, located near the wings, the airplane engine was severed from the fuselage, ending up outside the opposite facade that is facing Via Fabio Filzi.

The damage caused to the structures (Migliacci & Acito 2003, Migliacci et al. 2004b, Acito & Migliacci 2004) on the 26th floor indicated cracks at mid span of the longitudinal beams as well as at the fixed ends and along the border of the thin r.c. slab above the beams (Fig. 5). That damages result in conspicuous displacements at mid span of the beams, ranging from a maximum of 25 cm of beam No. 5 to 14 cm of beam No. 1 (Fig. 6).

As regard to the deck of the 27th floor, the deformation evidenced an upward residual displacement

of 5–6 cm at mid span of beam No. 5, the most severely damaged one, confirming the hypothesis that the impulse due to the explosion of the gasoline tanks was the major cause of the permanent displacements.

The problem of the realignment of the beams of the 26th deck appeared to be of fundamental importance



Figure 1. Pirelli building before and after the crash.

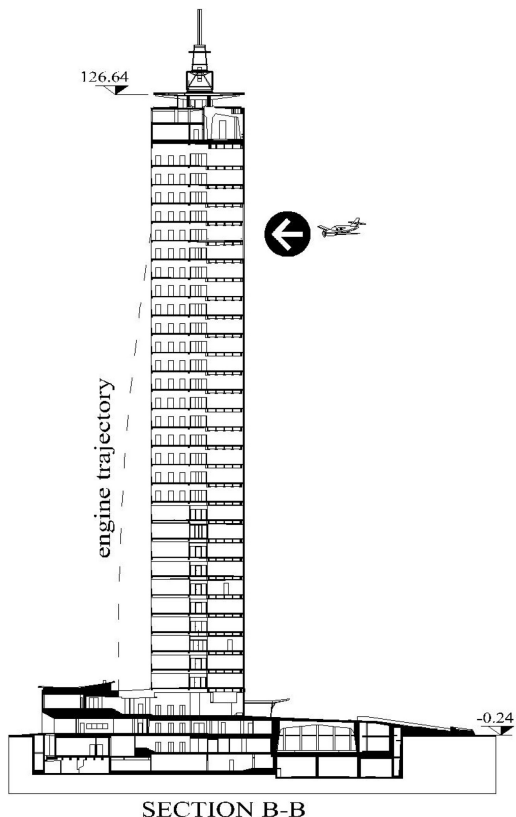


Figure 2. Longitudinal section of the Pirelli building.

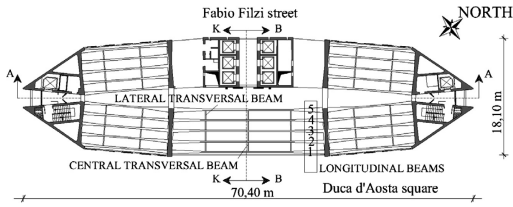


Figure 3. Floor plan of the Pirelli building.

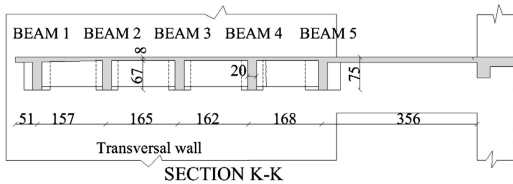


Figure 4. Floor section of the Pirelli building.



Figure 5. Yield lines after concrete demolition.

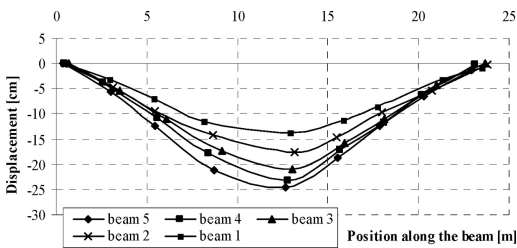


Figure 6. Residual displacements of the 26th floor beams.

inasmuch as the mandate from the owner (Public Administration of Lombardia Region) was to attempt to preserve the existing structures. With this in mind, it was essential to force the beams upwards by using hydraulic jacks on a pack prop.

As the sequel of this paper will show, achievement of this objective was made possible by relying on plastic displacement set up in the opposite direction in relation to the configuration after the explosion. Moreover, the reasoning was that it should be possible to arrive to a simple analytical model for estimating the forces

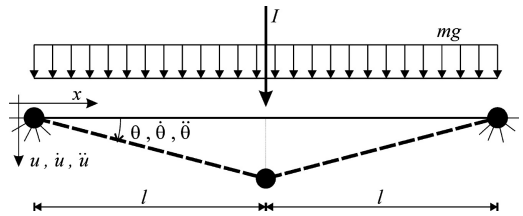


Figure 7. Plastic hinges model of a generic beam of the deck.

required for such a forcing process; such an estimation would be necessary in order to make a suitable choice of the jack types to be utilized on the field.

2 ANALYTICAL EVALUATION OF THE IMPULSIVE LOADING DISTRIBUTION

The analytical evaluation of the impulsive loading distribution which has caused the deformed configuration of the 26th and 27th floors has been determined with a procedure similar to that of a back analysis: knowing the permanent displacements distribution of the floors, the load are evaluated back.

2.1 Rigid plastic dynamic model

A simple rigid plastic dynamic model (Hodge 1959, Franchi et al. 1998) has been implemented as a possible tool for evaluating the response of reinforced concrete beams under blast loading. This model of a generic beam is based on a three plastic hinges scheme connecting two rigid elements (Fig. 7). The description of the kinematics of the system is expressed in terms of rotation, rotation velocity and rotation acceleration of the plastic hinge placed at the end of the beam.

By assuming that the initial conditions of motion ($t = 0$ s) are characterised by zero rotation and rotation velocity of the plastic hinges and by calling with A the cross section area of the beam, with ρ its density and with m its mass for unit length, the definition of impulse loading I reads:

$$I = 2 \int_0^l A \rho \dot{\theta}_0 x dx = m l^2 \dot{\theta}_0 \quad (1)$$

where l is the length of the rigid link between two plastic hinges (half of the total length of the beam).

By assuming that the motion after the blast is a free damped motion in which the rotational acceleration of the plastic hinge can be considered constant, its value can be determined by imposing that, during the motion, the sum of kinetic energy K , load potential U and energy dissipated D is constant, or, in terms of rate quantities:

$$\dot{K} - \dot{W} + \dot{D} = 0 \quad (2)$$

Table 1. Beams data.

Beam	$2l$ m	b m	m kg/m	M_S^+ kNm	M_S^- kNm	M_E^+ kNm	M_E^- kNm
1	24.69	1.31	982	945	226	785	1289
2	24.54	1.61	963	948	226	787	1280
3	24.43	1.63	963	948	226	787	1280
4	24.39	1.63	963	948	226	787	1280
5	24.09	2.46	1543	1175	269	923	1819

where $W = -U$ is the load work. By expressing K , W and D as:

$$\dot{K} = 2 \int_0^l m \ddot{u} \dot{u} dx; \dot{W} = 2 \int_0^l m g \dot{u} dx; \dot{D} = 2(M_S^+ + M_E^-) \dot{\theta} \quad (3)$$

where M_S^+ and M_E^- are the absolute values of the mid span positive (bottom fibres in tension) and fixed end negative ultimate moments, determined at steel yielding in tension, and g is the gravity acceleration.

The time t_f required to stop the dynamic process can be determined on the basis of the value of the rotational acceleration obtained from the solution of equation (2). The mid span final displacement u_f^+ measured at time t_f (Franchi et al. 2005), positive if downward, is:

$$u_f^+ = \frac{I^2}{m[6(M_S^+ + M_E^-) - 3mgl^2]} \quad (4)$$

In the same way the mid span final displacement u_f^- of a beam which has an impulse force from the bottom to the top may be expressed as:

$$u_f^- = -\frac{I^2}{m[6(M_S^- + M_E^+) + 3mgl^2]} \quad (5)$$

where M_S^- and M_E^+ are the absolute values of the mid span negative and fixed end positive ultimate moment respectively.

2.2 Blast loading distribution

The essential data required for the determination of the blast impulse are resumed in Table 1 for the various beams (Nervi 1960, Ponti 1960). They are: span $2l$, influence width b , mass per unit length m (comprising self weight and dead loads) and ultimate moments.

The blast impulse caused by the explosion on the beams of the 26th and 27th floor of the building can be determined by means of the equations (4) and (5) starting from the measured permanent deflections of the beams. The computed impulses range from 28 to 60 kNs in downward direction, on the 26th deck, and from 6 to 9 kNs in upward direction on the 27th floor (Tables 2 and 3).

The blast pressure can be assumed as a triangular pulse characterised by a peak pressure p_m and a duration t_d (see Fig. 8). The consequent blast impulse I is measured by the area under the time-force curve:

$$I = (p_m t_d A) / 2 \quad (6)$$

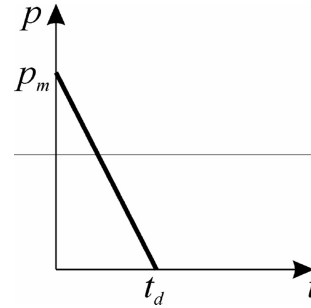


Figure 8. Blast impulse pressure during time.

Table 2. Blast impulses and peak pressures on 26th floor.

Beam	u_f^+ mm	I kNs	A m ²	P_m MPa
1	90	28.20	10.7	4.04
2	130	33.76	13.1	3.96
3	165	38.11	13.3	4.42
4	185	40.39	13.3	4.69
5	207	60.29	19.8	4.70

Table 3. Blast impulses and peak pressures on 27th floor.

Beam	u_f^- mm	I kNs	A m ²	P_m MPa
1	-22	6.00	10.7	0.86
2	-24	6.47	13.1	0.76
3	-35	7.90	13.3	0.92
4	-45	8.99	13.3	1.04
5	-63	7.42	19.8	0.58

where A is the influence area of the floor on which the pressure is considered constant, assumed equal to the influence width b times one third of the span of the beam.

Assuming that the blast duration t_d is 1.3 ms (Ngo et al. 2007) and knowing the blast impulse I , the peak pressure can be calculated from equation (6). The distribution of blast impulses and peak pressures on the various beams is presented in Tables 2 and 3. It is important to remark that only the plastic part of the displacements u_f^+ and u_f^- has been used in these calculations, according to the rigid-plastic hypothesis assumed in the described analytical model.

The obtained peak pressures are about 4 MPa in downward direction on the 26th floor with a distribution showing higher values in correspondence of the inner beams (No. 4 and 5). Lower values (about 1 MPa) are applied in the upward direction on the 27th deck.

3 REALIGNMENT OF THE 26TH FLOOR

It has been recognized that the first operation to be carried out, before any type of consolidation of the

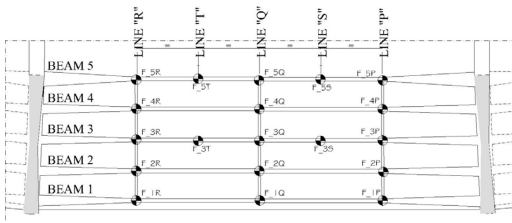


Figure 9. Hydraulic jacks distribution.

structures, had to be the realignment of the principal beams of the 26th floor. Only after the realignment, in fact, it is conceivable to remove the damaged concrete (class C20/25), substitute those parts of the bars which did suffer inelastic strains especially in compression (Park et al. 1982), reconstruct the concrete sections with special self-compacting mortar ($f_{ck,cube} = 49$ MPa), and finally to apply a post-tensioning steel system which will increase the safety level of the repaired structure.

3.1 Operative procedure

The operative procedure had to employ N. 15 hydraulic jacks (see Fig. 9) positioned at the intersection of the 5 longitudinal beams with the 3 transversal beams; other 4 jacks were added in between the previous points, only for beam No. 3 and 5, in order to better distribute the uplift loads, especially for the most damaged beams.

The jacks were placed in contact to the bottom face of the beams by means of provisional steel beams fixed to the floor. Close to the jack points some steel tubular props follow the realigning process, by adapting their height, step by step, following the movements of the beams.

The idea was that to force the beams up to collapse in the upward direction and then to move the mid span section of each beam over the horizontal line of a displacement equal to the elastic displacement caused by the same 3 point loading forces.

The evaluation of the upward loads to be applied in order to obtain the realignment can be made by another simple model made of three plastic hinge connected by rigid elements. The required displacement, upward the horizontal line, in order to obtain a flat floor after removal of the applied uplift forces can be determined too.

3.2 Analytical model for the evaluation of the total realignment force

The simple model adopted for the realignment process is shown in Figure 10. The applied forces are three point loads equal to $F/3$, representing the action of the hydraulic jacks, and the self weight mg per unit length, the other quantities follows the same notation of the previous paragraphs.

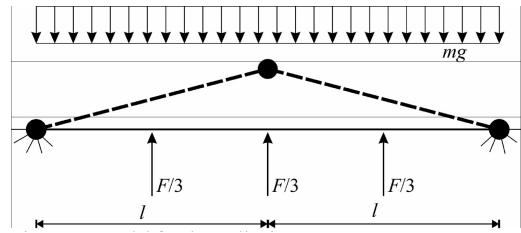


Figure 10. Model for the realigning process.

The limit load for the forcing up of the beams of the 26th floor F_u may be expressed as:

$$F_u = \frac{3(M_E^+ + M_S^-)}{l} + \frac{3}{2} mgl \quad (7)$$

By applying equation (7) to the five beams of 26th floor and summing the obtained forces, a total force of about 2600 kN is obtained. The experimental results proved the goodness of the assumptions.

3.3 Evaluation of the displacement

The model for the evaluation of the beams deflection of the 26th floor in service conditions was that of a fixed end beam subjected to uniform distributed load of 10 kN/m. The mid span displacement measured by means of experimental tests is around 2 cm, for a corresponding average elastic stiffness $EJ = 432000$ kNm², comprised between the un-cracked and fully cracked stiffness.

The actual elastic stiffness, reduced by the degradation due to the explosion and the realigning process, should be assumed about half the original, i.e. 200000 kNm², due to the fact that only the critical sections suffered limited damages.

By assuming a fixed end beam subjected to three point loads equal to $F/3$, the elastic displacement f at mid span up to the horizontal line will be:

$$f = \frac{Fl^3}{36EJ} = \frac{493 \cdot 12^3}{36 \cdot 200000} = 0.118\text{m} \quad (8)$$

Therefore the target displacement during the uplift process for beam No. 5 was fixed into 12 cm.

3.4 Realignment process

Forcing operations have been obtained by applying the uplift loads F evaluated in section 3.2. The load control system consisted of an oil distributor which controlled, through suitable valves, the oil flow in each jack. The sequence of the loading history has been organized so that the final load was subdivided into steps: inside each loading step, single beams have been loaded one after the other starting from No. 5 to finish with No. 1. The loading of each single beam has been obtained, at each loading step, by increasing the lateral loads and keeping the central load constant, and then vice versa,



Figure 11. Prop and hydraulic jacks at beam No. 3.

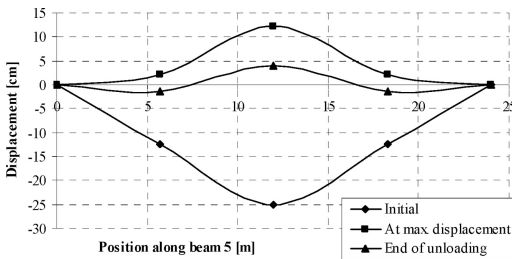


Figure 12. Displacement monitoring during forcing process.

i.e. increasing the central load by keeping the lateral loads constant.

The 25th, 24th, 23rd and 22nd floors have been stiffened provisionally by pack props in order to distribute on four floors the total uplift load applied to the 26th deck, such that each floor would take no more than the allowable service load.

The displacement monitoring system was made of No. 15 displacement electrical transducers connected to a digital data acquisition system. The displacement transducers were located between the 26th and 27th floor, by considering the 27th floor as a fixed reference system. The total time required for the realigning process was about 30 hours. Figure 11 shows a picture of the hydraulic jacks and props system, while Figure 12 shows the real time displacement diagram during forcing phase.

A picture of the mid span plastic hinge of beam No. 5 during the final stages of the process is shown in Figure 13. It is remarkable the buckled configuration of the compressed bars.

4 STRENGTHENING OF THE BEAMS BY MEANS OF POST-TENSIONING TENDONS

4.1 Post-tensioning design

A post-tensioning system, acting on the 5 damaged beams of the 26th floor, has been conceived in order to improve the flexural stiffness of the entire floor (Migliacci et al. 2004a).



Figure 13. Plastic hinge at mid span of beam No. 5.

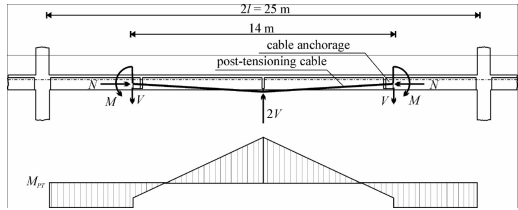


Figure 14. Post-tensioning geometry, equivalent loads and bending moments.

The system is made, for each beam, of two post-tensioned cables (each one made of 5 strands of 0.6" , placed on one side of the beam) acting as a reverse arch, with the anchorages located near the transverse beams and the crown in the middle of the longitudinal beams where the cable deviation device is positioned. The post tensioning cable inclined geometry is presented in Figure 14 together with the system of static loads equivalent to the post-tensioning action. Axial N , shear V and bending M actions are applied in correspondence of the anchorage, while, due to the particular selected geometry of the cable, an upward load $2V$ is applied in the middle of the beam. The bending moment diagram induced by post-tensioning on the statically indeterminate scheme of the longitudinal beam, with built-in ends in the core walls of the tower, is also shown. The diagram shows the goodness of the designed post-tensioning in order to carrying on the applied load.

The architectonic implications have been also considered in the selection of the tendon geometry.

4.2 Anchorage devices: "noses"

The tension load present in the cable is transferred to the longitudinal beam by means of a couple of anchorage devices, placed at both sides of the beam web. The anchoring devices, named "noses", are made of a particular reinforced concrete characterised by an high workability, cast in place in a stainless steel (AISI 304) formwork. The idea is that to fix the noses to the sides of the beam web, as is usually done in the external cables post-tensioning system, by means of another post-tensioned joint.

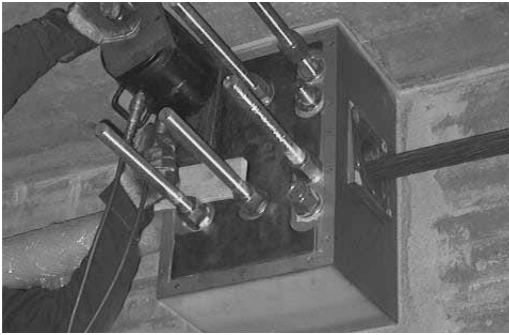


Figure 15. Tensioning of the threaded bars fixing the nose to the side of the longitudinal beams.

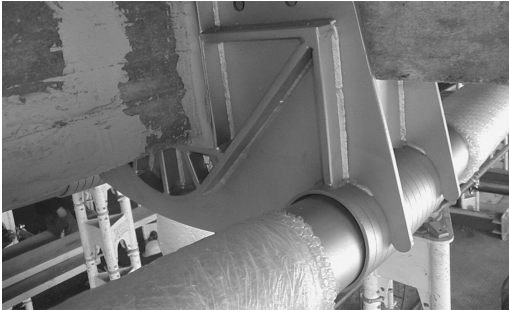


Figure 16. Cables deviation device.

The monolithic connection between noses and beam is realized by the tensioning of 8 threaded bars which cross the beam web, in which has been previously drilled 8 holes, and the two noses placed on its sides, connecting each other (Fig. 15). The threaded bars are made of duplex stainless steel with a yield strength of $f_{yk,0.2} \geq 700$ MPa and a 30 mm diameter.

4.3 Deviation device

The device placed in the middle of the longitudinal beam which allows the deviation of the post-tensioning cables, developing the vertical sustaining load $2V$, is made of stainless steel (AISI 304) welded plates having the particular geometry shown in Figure 16.

5 CONCLUSIONS

The realigning process has requested, or stimulated, to solve several problems and, among the others, the following are the most significant:

- the evaluation of the impulse and peak pressures distribution during the explosion of the aircraft tanks which has caused the severe damages of the structures of the 26th and 27th reinforced concrete floors;

- the evaluation of the total force to be applied by hydraulic jacks in order to obtain the realignment of the 26th floor;
- the evaluation of the maximum displacement over the horizontal line necessary in order to obtain a flat plane after removal of the forcing jacks action, with a maximum error of 2–3 cm;
- the operative technique able to implement and to control the forces and displacements during the realigning process;
- the design of a post-tensioning system of external cables capable to increase the strength of the damaged beams of the 26th deck, comprising the anchorage and deviation devices;
- the restoration of the plastic hinges sections in the middle and at the end of the beams with concrete and reinforcing steel similar to the original one.

ACKNOWLEDGEMENT

The authors acknowledge the high professional skills of P&P Consulting Engineers, ISMES-LMC and Grassi & Crespi technical staff which has greatly contributed to the success of the whole operation.

REFERENCES

- Acito, M. & Migliacci, A. 2004. Il progetto e la tesatura dei cavi nel risanamento strutturale dell'impalcato del 26° piano del grattacielo Pirelli. *Congresso AICAP*, Verona.
- Franchi, A., Acito, M., Crespi, P. & Migliacci, A. 2005. Analytical and experimental procedures for the realigning of the 26th floor of the Pirelli tall Building after the air-plane crash on April 2002. *Proc. IABSE International Symposium, Lisbon, Portugal, 14–16 September 2005*.
- Franchi, A., Genna, F. & Corradi, L. 1998. On the determination of bifurcation and limit points. *Journal of Engineering Mechanics*, 124 (8): 866–874.
- Hodge, P.C. 1959. *Plastic Analysis of Structures*. Mc Graw Hill.
- Migliacci, A. & Acito, M. 2003. *La Vicenda del grattacielo Pirelli – il restauro*. Roma: Mancosu Editore.
- Migliacci, A. et al. 2004a. Modelli numerici per l'interpretazione del comportamento del c.a. in regime non lineare: la vicenda del grattacielo Pirelli. *Congresso CTE, Bari, Italy*.
- Migliacci, A., Acito, M. & Franchi, A. 2004b. Il progetto di risanamento delle strutture del grattacielo Pirelli. *Studies and Researches V. 24*. Italcementi S.p.A., Bergamo.
- Nervi, P. 1960. L'ossatura. *Edilizia Moderna*, n. 71.
- Ngo, T., Mendis, P., Gupta, A. & Ramsay, J. 2007. Blast Loading and Blast Effects on Structures – An Overview. *EJSE Special Issue: Loading on Structures*: 76–91.
- Park, R., Priesley, M.J.N. & Gill, W. D. 1982. Ductility of Square Confined Concrete Columns. *Journal of the Structural Division, ASCE Vol.108 n°ST4*: 929–950.
- Ponti, G. et al. 1960. Il Progetto. *Edilizia Moderna*, n. 71.